


5-2016

# Exploring the Black Space of Compressive and Shear Modulus

Airam Marlee Morales Vega  
*University of Arkansas, Fayetteville*

Follow this and additional works at: <http://scholarworks.uark.edu/etd>

 Part of the [Civil Engineering Commons](#), and the [Transportation Engineering Commons](#)

---

## Recommended Citation

Morales Vega, Airam Marlee, "Exploring the Black Space of Compressive and Shear Modulus" (2016). *Theses and Dissertations*. 1496.  
<http://scholarworks.uark.edu/etd/1496>

This Thesis is brought to you for free and open access by ScholarWorks@UARK. It has been accepted for inclusion in Theses and Dissertations by an authorized administrator of ScholarWorks@UARK. For more information, please contact [scholar@uark.edu](mailto:scholar@uark.edu), [ccmiddle@uark.edu](mailto:ccmiddle@uark.edu).

# Exploring the Black Space of Compressive and Shear Modulus

A thesis submitted in partial fulfillment  
of the requirements for the degree of  
Master of Science in Civil Engineering

by

Airam Marlee Morales Vega  
Technological University of Panama  
Bachelor of Science in Civil Engineering, 2013  
Technological University OTEIMA  
Master in Education, 2014

May 2016  
University of Arkansas

This thesis is approved for recommendation to the Graduate Council.

---

Dr. Andrew Braham  
Thesis Director

---

Dr. Gary Prinz  
Committee Member

---

Dr. Sarah Hernandez  
Committee Member

## **Abstract**

Uniaxial dynamic modulus is a standard test used to determine the viscoelastic behavior of asphalt pavement materials, with the standard analysis generating a Master Curve. One alternative to the master curve approach is a Black Space diagram, which is a rheological plot that can delineate either dynamic modulus  $|E^*|$  or shear modulus  $|G^*|$  vs. phase angle ( $\delta$ ). In this study, four asphalt binders were tested with one aggregate blend. One of these four binders was unmodified and the other three were modified with polymers and acids. Additionally, Polyphosphoric acid (PPA) is compared to the more traditional SBS polymer modification. PPA is currently prohibited in Arkansas because of a lack of information on its field performance. Three tests were performed: Uniaxial  $|E^*|$ , Indirect Tension (IDT  $|E^*|$ ), and Torsion Bar  $|G^*|$ . Traditional Master Curves and Black Space diagrams were plotted to have a comparison between all materials. The results show that Black Space diagram plotted with the Torsion Bar  $|G^*|$  configuration is able to more clearly identify viscoelastic behavior of asphalt pavement materials in comparison with the master curve approach.

## **Acknowledgements**

I would like to thank my family and my friends for their affection and support.

Also, to my advisor Dr. Andrew Braham, for giving me the opportunity to do research and for all of his advice during Graduate School. Additionally, thanks to my committee members Dr. Gary Prinz and Dr. Sarah Hernandez for their guidance.

Thanks to Shu Yang and Elvis Castillo for their support and for sharing your knowledge and great moments with me.

Thanks to Leslie Parker, Anabella Monterroso, Martin Bonilla, and Allyson Richey for doing an amazing job in the asphalt laboratory.

To Arkansas State Highway and Transportation Department (AHTD), thanks for providing the materials used for this research through the project TRC 1501 “Performance of Asphalt Modified with Polyphosphoric Acid (PPA).” Also, to Dr. Zahid Hossain from Arkansas State University for his guidance during this research.

## **Dedication**

This thesis is dedicated first of all to God Almighty for giving me the strength to keep going.

To my parents, María and José, for being supportive in every decision I made.

To my brother, Josimar, for his words of encouragement.

And finally to my boyfriend, Edgar, for being there always I need him.

## Table of Contents

I.	Introduction .....	1
II.	Background.....	4
A.	Black Space Diagram .....	6
B.	Dynamic Modulus vs. Shear Modulus .....	7
C.	Asphalt Modifiers .....	8
III.	Materials and Methods.....	10
A.	Materials .....	10
B.	Laboratory Testing .....	11
IV.	Results.....	16
A.	Master Curves.....	17
B.	Black Space Diagram .....	20
C.	Statistical Test.....	22
V.	Discussion.....	24
VI.	Conclusions.....	24
	References.....	26

## List of Tables

Table 1. Proposed Geometry and Samples to perform Black Space Diagram .....	11
Table 2. Test Matrix.....	13
Table 3. ANOVA and Tukey's Method for $ E^* $ Dynamic Modulus.....	23
Table 4. ANOVA and Tukey's Method for phase angle.....	24

## List of Figures

Figure 1. Most common asphalt concrete pavements' distresses: cracking and rutting (by author)	2
Figure 2. Example of a Black Space Diagram for mixture - $ E^* $ vs. phase angle (from Mensching et al., 2015) .....	6
Figure 3. Black Space Diagram of a Plant vs. Laboratory (from Rastegar, 2016) .....	7
Figure 4. Components of Complex Modulus $G^*$ .....	8
Figure 5. Dynamic Modulus master curve (from Li et al., 2011).....	9
Figure 6. Uniaxial $ E^* $ Geometry .....	12
Figure 7. Indirect Tensile (IDT $ E^* $ ) Geometry .....	12
Figure 8. Torsion Bar $ G^* $ Geometry .....	12
Figure 9. Uniaxial $ E^* $ Test .....	14
Figure 10. IDT $ E^* $ Setup .....	15
Figure 11. Torsion Bar $ G^* $ Setup .....	16
Figure 12. Uniaxial $ E^* $ Dynamic Modulus Master Curve .....	18
Figure 13. IDT $ E^* $ Dynamic Modulus Master Curve.....	19
Figure 14. Torsion Bar $ G^* $ Master Curve .....	19
Figure 15. Torsion Bar $ G^* $ in Log Configuration Master Curve .....	20

Figure 16. Uniaxial $ E^* $ Dynamic Modulus Black Space Diagram .....	21
Figure 17. IDT $ E^* $ Black Space Diagram .....	21
Figure 18. Torsion Bar $ G^* $ Black Space Diagram .....	22



## **I. Introduction**

Asphalt pavement is commonly used in transportation roads because of its beneficial properties and characteristics. For instance, asphalt roads can be built easily with a low cost, in comparison with other materials, and provide a smooth and safe quality riding surface (Wagoner *et al.*, 2005). Every year, a significant amount of money is invested in designing, constructing, and maintaining asphalt pavement, due to external factors such as traffic loads, environmental conditions, construction practices and material properties that can deteriorate asphalt pavement (Behbahani *et al.*, 2013).

Fatigue cracks, (Figure 1a) which are created by traffic loading, generally form at the bottom of the asphalt layer, where the tensile stress and strain are the highest, and propagate upward to the surface with repeated traffic loads (Khattak, 2013). Consequently, it is necessary to rehabilitate the pavement when the riding surface is unacceptable (Mobasher *et al.*, 1997). Rutting, also results from traffic loads. For instance, (Figure 1b) shows a permanent path into the pavement. Other factors, such as deformation of the subgrade and erosion, contribute to rutting (Cao *et al.*, 2016). Cracking is often associated with the elastic characteristics of a material (higher elasticity tends to lead to more cracking), while rutting is often associated with the viscosity characteristics of a material (higher viscosity tends to lead to more rutting).



a) Fatigue Cracks



b) Rutting

**Figure 1. Most common asphalt concrete pavements' distresses: cracking and rutting (by author)**

In order to determine the properties of the asphalt concrete materials, which are viscoelastic in nature, various tests and analysis techniques are often used. For example, the Dynamic Modulus  $|E^*|$  Test can define the asphalt mixtures' response in both elastic and viscous components.  $|E^*|$  is defined as the material stiffness and is reliable to identify distresses like cracking and rutting in asphalt pavements (Naik *et al.*, 2014). Master curves are used to analyze the data obtained from complex modulus test. The purpose of the master curves on asphalt mixtures is to compare wider the ranges of temperatures or frequencies. Master curves uses the principle of superposition which permits that the data measured from the test at different temperatures and frequencies can be shifted in a horizontal way and consequently lined up to form a master curve (Clyne *et al.*, 2003).

A Black Space diagram can delineate a dynamic modulus such as shear modulus ( $G^*$ ) and phase angle ( $\delta$ ) (Romero, 2013). Phase angle ( $\delta$ ) in a visco-elastic material like asphalt which can be

defined as the “time delay of a material’s reaction to an applied load during a sinusoidal type test” (Romero, 2013). The complex shear modulus  $G^*$  “is a complex number that is defined by the ratio of shear stress to shear strain” (ASTM, 2014). The complex modulus  $E^*$  “is a complex number that defines the relationship between stress and strain for a linear viscoelastic material” (AASHTO, 2014). Additionally, Black Space diagram is a rheological tool which is beneficial to evaluate elasticity and stiffness of a material by using or not the time-temperature superposition in order to transform to the reduced frequency (Menching *et al.*, 2015). The values for Black Space diagram can be measured in a uniaxial form from the Dynamic Modulus (AASHTO T 342) test, and in the Indirect Tensile form from the Indirect Tension Test, IDT  $|E^*|$ , (Kim *et al.*, 2004) using the samples configuration from AASHTO T 322. This study looks to generate Black Space diagram by obtaining the shear linear viscoelastic modulus ( $|G^*|$ ) in the torsion bar configuration and the dynamic linear viscoelastic modulus ( $|E^*|$ ) in both the uniaxial and indirect tension configuration.

In addition to exploring the Black Space diagram, this study includes the evaluation of the effects of Polyphosphoric Acid (PPA), which is a polymer that modifies a neat asphalt binder in order to improve asphalt concrete performance (Baumgarder *et al.*, 2010). There are some concerns in the state of Arkansas about the usage of PPA as a modifier binder due to uncertainties about how it reacts with other polymers and its effects on the environment (Li *et al.*, 2011). The results of this study will contribute information to the state of Arkansas on the usage of PPA.

The objectives of this paper are:

- Test the shear dynamic modulus from the torsion bar test ( $|G^*|$ ) and dynamic modulus from uniaxial and indirect tension (uniaxial  $|E^*|$  and IDT  $|E^*|$ ) at different temperatures and frequencies.

- Investigate the relationship between the Shear Modulus ( $|G^*|$ ) and phase angle ( $\delta$ ) by creating a Black Space diagram.
- Compare the relationship between  $|E^*|$  and  $|G^*|$  plotted in Master Curves and Black Space diagram.
- Investigate the effects that PPA and other polymers have in the values calculated for Black Space diagram.

## II. Background

Elasticity is a behavior of many materials used in Civil Engineering. An elastic response occurs when a material experiences deformation while an external force is applied, but because the material is not damaged, the deformation fully recovers when the force is removed. Stress and strain are two common measurements used to quantify linear elastic materials. Stress is a physical quantity that represents the internal force, whereas strain measures the deformation (Timoshenko, 1953).

Understanding the relationship between stress and strain at different temperatures and loading frequencies in asphalt pavements is necessary to obtain a satisfactory pavement design and analysis. Theories of elasticity, viscoelasticity, and elasto-visco-plasticity have been used to analyze flexible pavements. Westergaard, in 1927, first used the elastic theory to analyze Portland cement concrete pavements (Taherkhani *et al.*, 2008). Then, Burmister, in 1943, established an elastic theory for a two-layer pavement (Taherkhani *et al.*, 2008). This theory explains that the materials which are comprising the layers are assumed to be homogenous, isotropic, and linear elastic. For elastic analysis, the principal parameters used are the Elastic Modulus and Poisson's Ratio. These parameters can also be used for other analysis in viscoelastic and elasto-visco-plastic. These values in asphalt concrete are frequently found using

empirical values or theoretical equations. Other models were used for asphalt concrete characterization, including stress and strain analysis and rutting predictions in asphalt pavements. This model, which includes non-linear effects, is called the linear viscoelastic model (Taherkhani *et al.*, 2008).

The dynamic modulus test, which finds  $|E^*|$ , is useful to characterize the stress/strain behavior in the asphalt concrete pavements. The purpose of this test is to simulate the traffic loads and the deformation caused on the pavements (Yang *et al.*, 2015). Papazian, in 1962, described how the viscoelastic test was performed on asphalt pavement. In order to measure the dynamic modulus (Eq.1), a sinusoidal stress was applied to a cylindrical specimen with an established frequency and it also measured a sinusoidal strain using the same frequency. Additionally, the test considers using different given frequencies and controlled temperatures. Uniaxial dynamic modulus  $|E^*|$  test is the standard test used in material characterization, so it is not considered a new concept for asphalt mixtures. Consequently, after more than 50 years, researchers still use these concepts (Clyne *et al.*, 2003).

$$|E^*| = \frac{\sigma_o}{\varepsilon_o} \quad (1)$$

Where:  $\sigma_o$  is stress and  $\varepsilon_o$  is strain.

However, many of these empirical values, equations, and laboratory experiments can be both time consuming and require significant laboratory equipment. Therefore, it is worth exploring ways to plot Black Space diagram in order to gain additional data and information from existing data collected from dynamic modulus. One such relationship exists between the shear modulus, the elastic modulus and the phase angle (Di Benedetto *et al.*, 2004).

## A. Black Space Diagram

Black Space diagram, which represents a plot of complex stiffness modulus versus phase angle, is used usually as a rheological tool that helps to evaluate material properties such as stiffness and elasticity associated by using or not using the time-temperature superposition principle in order to transform decreased frequency or time domain (Mensching *et al.*, 2015).

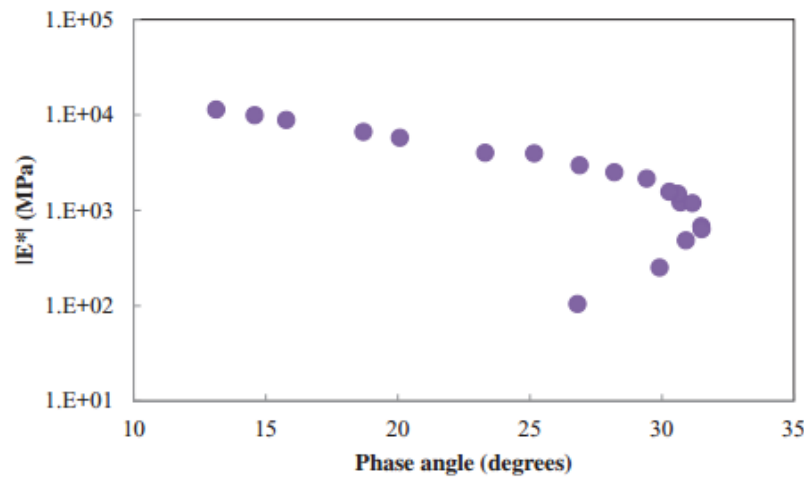


**Figure 2. Example of a Black Space Diagram for mixture -  $|E^*|$  vs. phase angle (from Mensching *et al.*, 2015)**

Black Space diagram can be related to low-temperature feature due to the fact that phase angle illustrates the relaxation. Figure 2 shows a Black Space diagram for a mixture where a peak phase angle value for stiffness is seen because of the combination of asphalt binder and the aggregate. Therefore, at high temperatures the aggregate structure starts to control its behavior because the asphalt binder presents low stiffness and viscous flow. At low temperatures other factors, such as mix volumetrics, aggregate, and binder stiffness, dominate behavior (Mensching *et al.*, 2015).

Figure 3 gives a plot of a Black Space diagram where laboratory and plant design is compared. This figure indicates how a Black Space diagram can be interpreted. For instance, if the diagram

of the mixture has a low phase angle value, it represents that the mixture is more elastic. On the other hand, if the phase angle is high, the mixture is more viscous. For a stiffer mixture, the dynamic modulus should be high (Rastegar, 2016).

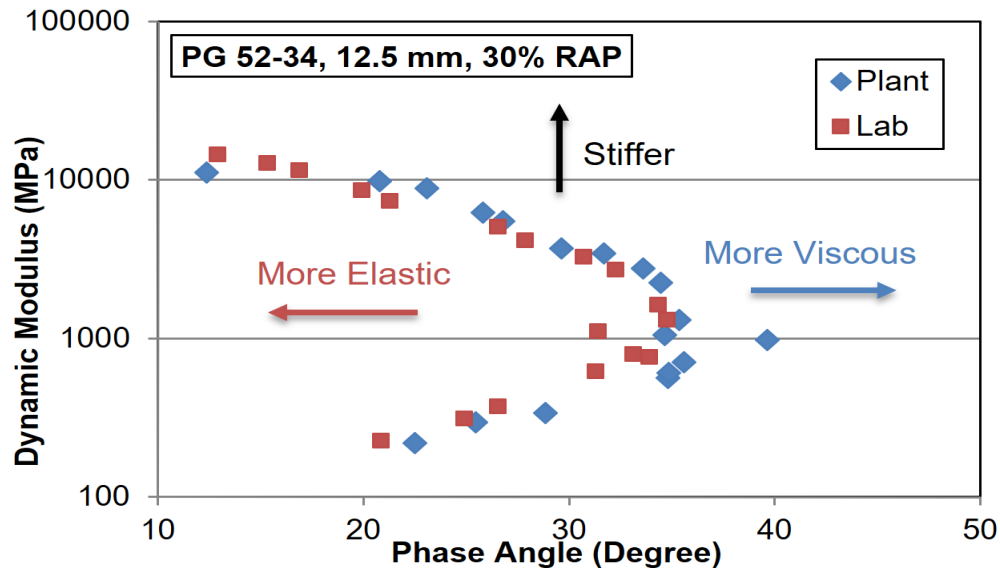
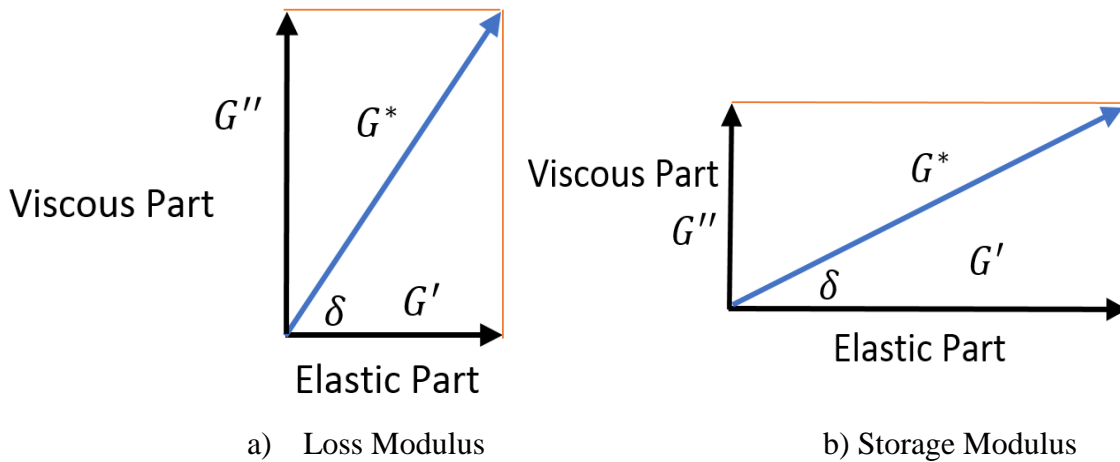


Figure 3. Black Space Diagram of a Plant vs. Laboratory (from Rastegar, 2016)

## B. Dynamic Modulus vs. Shear Modulus

In order to obtain the results for this research, Dynamic Modulus  $|E^*|$  from the uniaxial and indirect tensile configurations and Shear Modulus  $|G^*|$  from the torsion bar configuration were used. The dynamic modulus  $|E^*|$  and shear modulus  $|G^*|$  will obtain the master curves to characterize the asphalt concrete (AASHTO, 2014). For asphalt materials, the traditional test configuration is uniaxial (Yang *et al.*, 2015), run with AASHTO T 342. The Indirect Tensile configuration (IDT  $|E^*|$ ) does not have a specification, but Kim *et al.* (2004) implemented an analysis using indirect tensile mode in dynamic modulus. IDT  $|E^*|$  can be executed from 150 mm diameter sample from the laboratory or field (Yang *et al.*, 2015).

The geometry for torsion bar to obtain  $|G^*|$  is helpful for forensic assessment of pavements that are in-service, and one advantage is that this test can be used when there is not enough material for other tests (Yang *et al.*, 2015). Complex Shear Modulus  $G^*$  and phase angle ( $\delta$ ) are obtained from the Dynamic Shear Rheometer (DSR) which is used to characterize asphalt binder behavior, such as elastic and viscous. Figure 4 shows the components of Complex Modulus  $G^*$ . Figure 4a represents the storage modulus  $G'$  (G prime) which is the elastic recoverable part, and Figure 4b represents the loss modulus  $G''$  (double prime) which is the viscous non-recoverable part (Roberts *et al.*, 1996).



**Figure 4. Components of Complex Modulus  $G^*$**

### C. Asphalt Modifiers

In the United States, the use of polymers and acid as modifier binders are very popular because it is believed that they increase rutting and cracking resistance of asphalt concrete (Li *et al.*, 2011). Polyphosphoric Acid (PPA) is a polymer that modifies the asphalt concrete in order to improve its performance (Baumgarder *et al.*, 2010). In some states, such as Arkansas, the use of PPA is banned due to the lack of research on its effects combined with other polymers (Li *et al.*, 2011). In this research, the PPA effects in asphalt concrete and how it behaves depending on the test



results will be evaluated. Another examples of polymers and acid are the following: Styrene-Butadiene-Styrene (SBS), Liquid Anti-Strip (LAA), and Elvaloy.

Several researchers did studies using PPA alone and combined with other polymers in order to investigate its properties by performing Uniaxial  $|E^*|$  Dynamic Modulus. In 2011, Li *et al.*, used four modified asphalt binders to construct their mixtures. The unmodified binder type used was PG 52-34. The modified binder polymers used were: PPA, PPA + Elvaloy, SBS, and SBS + PPA. One of the purpose of this study was to make a stiffness comparison between the polymer modifications and chemical modifications. Figure 5 shows the results obtained for Uniaxial  $|E^*|$  Dynamic Modulus. The lowest dynamic modulus was obtained from the mixture modified with PPA + Elvaloy at high frequencies which is the low-temperature region. However, in low frequencies this mixture obtained higher dynamic modulus in the region of high temperature. The remaining three mixtures' dynamic modulus were very similar to each other in the high frequencies, but PPA has the lowest dynamic modulus between the three mixtures in the low frequencies.

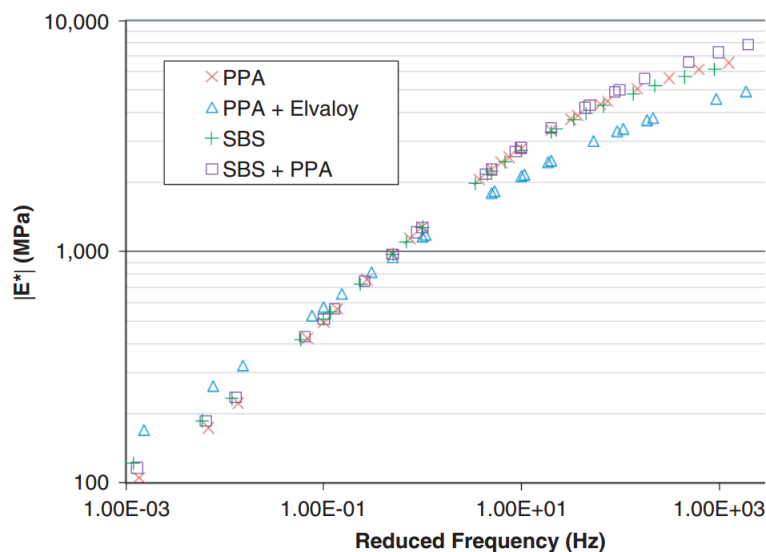


Figure 5. Dynamic Modulus master curve (from Li et al., 2011)

Moreover, Bennert *et al.*, in 2010, performed a Uniaxial  $|E^*|$  dynamic modulus test using SBS and PPA + SBS in their mixtures. The unmodified binder used was PG 64-22 and was modified to obtain PG 76-22. The results showed that in long term oven aging, the dynamic modulus were similar for both mixtures. Nonetheless, in short term oven aging, SBS + PPA showed slightly higher modulus than the SBS.

Another study, by Clyne *et al.*, in 2012, used a binder of PG 58-34 combined with 0.75% PPA only, 0.3% PPA + 1.0 % SBS polymer, 2.0% SBS polymer only, and 0.3% PPA + 1.1% Elvaloy polymer. The results showed that PPA + Elvaloy had the higher dynamic modulus at low frequencies and the lowest dynamic modulus at the highest frequencies. The remaining combinations had similar results. However, the SBS + PPA combination had higher dynamic modulus in the high frequencies.

### **III. Materials and Methods**

#### **A. Materials**

In order to study the benefits from the Black Space diagram, various mixtures were tested in the lab. To make a valid comparison, four binder types were used, where one binder type was unmodified and the other three were modified. Asphalt binder of PG 64-22, which is typically used in Arkansas, was used as the unmodified binder. In addition, three different acids and polymers were added to enhance the asphalt binder as listed below:

- PG 64-22 (unmodified base binder) = PG64
- PG 70-22 (base PG 64-22 modified with + 0.5% PPA) = PG70PPA
- PG 70-22 (base PG 64-22 modified with + 0.5% PPA + 0.5% LAA) = PG70PPAL

- PG 70-22 (base PG 64-22 modified with + 2% SBS) = PG70SBS

The aggregate used was 9.5 mm nominal maximum aggregate size which was collected from Van Buren, Arkansas. Aggregates such as 1/2” Chips, 3/8” VB Gr Chips, Manufactured Sand, 1/4” Screening, and Concrete Sand were used to make the mixture samples. The volumetric mix design is a fine graded mix because the gradation passes above the primary control sieve (PCS). The mix design properties of the binder were: 6.2% of optimal asphalt binder, 4.0% of air voids, 16% of VMA, 71.9% of VFA, and 1.26 fines to asphalt ratio.

## B. Laboratory Testing

Mixture samples were compacted in the laboratory with 7% air void for all four binder types and different geometries. Each geometry depends on the test performed. Therefore, Table 1 presents a test matrix with the geometries and tests that were performed.

**Table 1. Proposed Geometry and Samples to perform Black Space Diagram**

Test	Geometry	Volume (mm <sup>3</sup> )	Replicates
Uniaxial ( E* )	Diameter = 100 mm Height = 150 mm (Figure 6)	1,180,000	3 per binder
IDT  E*	Diameter = 150 mm Thickness= 38 mm (Figure 7)	672,000 2/ Uniaxial  E*	3 per binder
Torsion Bar  G*	12.5 mm x 6.5mm x 50mm (Figure 8)	4,100 288/ Uniaxial  E*	9 per binder



**Figure 6. Uniaxial  $|E^*|$  Geometry**



**Figure 7. Indirect Tensile (IDT  $|E^*|$ ) Geometry**



**Figure 8. Torsion Bar  $|G^*|$  Geometry**

The tests that were performed are the following:

**Table 2. Test Matrix**

Test	Source	Temperatures °C	Frequencies
Uniaxial $ E^* $ (Figure 9)	AASHTO T 342-11	-10, 4, 21, 37, and 54	0.1, 0.5, 1.0, 5, 10, and 25 Hz.
IDT $ E^* $ (Figure 10)	Kim <i>et al.</i> , 2004	-10, 4, 21, 37, and 54	0.1, 0.5, 1.0, 5, 10, and 25 Hz.
Torsion Bar $ G^* $ Figure (11)	ASTM D7552	-10, 0, 10, 20, 30, 40, 50, and 60	100, 63.1, 39.8, 25.1, 15.8, 10.0, 6.3, 4.0, 2.5, 1.6, 1.0, 0.6, 0.4, 0.3, and 0.2 rad/s .

- **Uniaxial Dynamic Modulus (AASHTO T 342-11):**

Uniaxial dynamic modulus test gives the values needed to measure the range of temperatures and loading frequencies in order to obtain master curves to help to characterize asphalt concrete (AASHTO, 2014). Therefore, a dynamic modulus test (Figure 7) was conducted on cylindrical specimens with a 100 mm diameter and a 150 mm height (Figure 6).



**Figure 9. Uniaxial  $|E^*|$  Test**

- **Indirect Tensile Test (IDT  $|E^*|$ ) (Kim *et al.*, 2004):**

The Indirect Tensile (IDT  $|E^*|$ ) does not have a specification. However, Kim *et al.* (2004) proposed an analysis in dynamic modulus using indirect tension mode. The Indirect Tensile (IDT) test was conducted on cylindrical specimens of 150 mm of diameter and 38 mm of height (Figure 8).

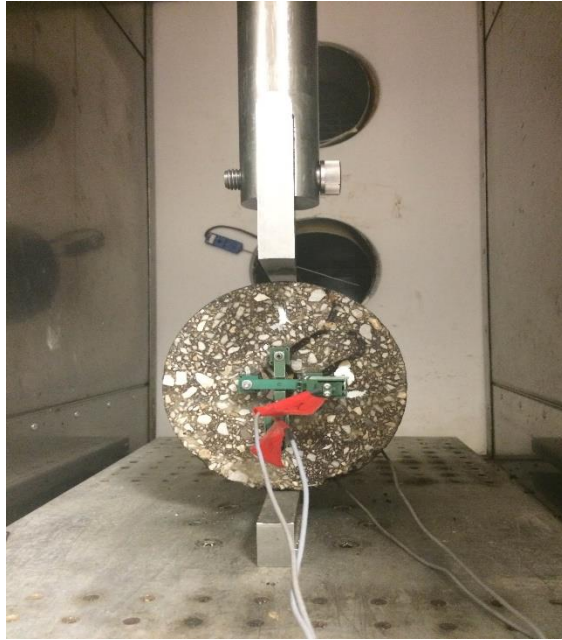


**Figure 10. IDT  $|E^*|$  Setup**

- **Complex Shear Modulus (ASTM D7552):**

The shear modulus is a material property of the asphalt concrete. Thus, the Dynamic Shear Rheometer is a test that gives the value of the Shear Modulus. Depending on the Shear Modulus value, the pavement will have a lower or higher deformation. In other words, mixtures will experience lower permanent deformation when they present higher shear modulus than the other mixtures that result in lower shear modulus values. The complex shear modulus used samples of 50 mm in length, 12.5 mm in width, and 6.5 mm in thickness (Figure 10).

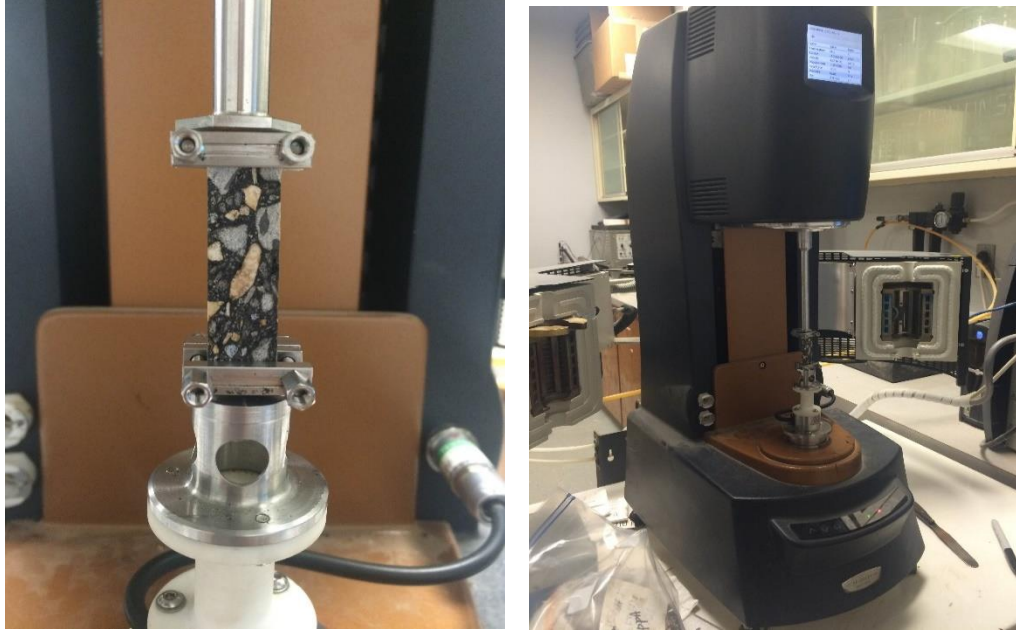


**Figure 11. Torsion Bar  $|G^*|$  Setup**

#### **IV. Results**

In order to make valid comparisons between the standard master curves and the Black Space diagram, the four binder types used were plotted in both methods. The master curves for Uniaxial  $|E^*|$  and Torsion Bar  $|G^*|$  were constructed based on AASHTO R 62 using the following coefficients for fitting the curves:  $\alpha = 3.0, \beta = -1.0, \delta = 0.5, \gamma = -0.5, a1 = 0.10,$  and  $a2 = 0.0010$ . For IDT  $|E^*|$  the master curves were first plotted using the same coefficients as AASHTO R 62, but the isotherms values were unreasonable because they did not overlap between temperatures. Therefore, it was used other coefficients proposed in the study by Yang *et al.*, 2015, for IDT  $|E^*|$  configuration, which are:  $\alpha = -1.1, \beta = 0.8, \delta = 4.0, \gamma = 0.4, a1 = 0.10,$  and  $a2 = 0.0010$ . The equation (Eq. 2) used for master curves is the following:

$$\log |E^*| = \delta + \frac{\alpha}{1 + e^{\beta + \gamma \log f_r}} \quad (2)$$



## A. Master Curves

For Dynamic Modulus  $|E^*|$ , both the Uniaxial and IDT tests have differences in the value ranges and plots. First, Uniaxial  $|E^*|$  plot (Figure 12) shows that for PG70SBS is stiffer than the other three binders in the low frequencies which is the high temperature region. However, in the high frequencies had the lowest dynamic modulus which is the low temperature region. It is interesting that the remaining mixtures which were PG64, PG70PPA, and PG70PPAL had very similar dynamic modulus along both regions. The values ranged from 350 MPa to 14,000 MPa. In comparison with the results of this study and the literature found, there are some differences. For example, in 2011, Li *et al.*, it was obtained very similar dynamic modulus between SBS and PPA mixtures. The behavior of PPA + Elvaloy (Figure 5) is more similar as the PG 70-22 + SBS behavior in this study.

Moreover, IDT  $|E^*|$  master curve (Figure 13) shows that the materials behave different than the Uniaxial  $|E^*|$ . The mixture PG64 had the lowest dynamic modulus in both low frequencies and high frequencies. For low frequencies, PG70PPA, PG70PPAL, and PG70SBS had very similar dynamic modulus. However, at high frequencies PG70SBS had higher dynamic modulus than PG70PPA, and PG70PPAL, which remain both very similar. The values ranged from 550 MPa to 10,000 MPa.

Furthermore, Torsion Bar  $|G^*|$  master curve (Figure 14) showed similar behavior as the IDT  $|E^*|$  results in the high frequencies region. The four materials have the same trending in the low frequencies. For instance, PG70SBS is stiffer than the other three materials in the high frequencies. For PG70PPA and PG 70PPAL, both graphs stayed in almost the same position. However, PG64 show a lower stiffness than the other materials in the high frequencies. The values ranged from 2 MPa to 7,000 MPa. The Torsion Bar  $|G^*|$  curves are also shown on a log-log plot (Figure 15) so

that differences in the low reduced frequency range can be more easily observed. In this figure, the difference in the SBS modified binder is apparent, while the PPA modified binders do not deviate from the neat binder behavior at higher temperatures and lower frequencies.

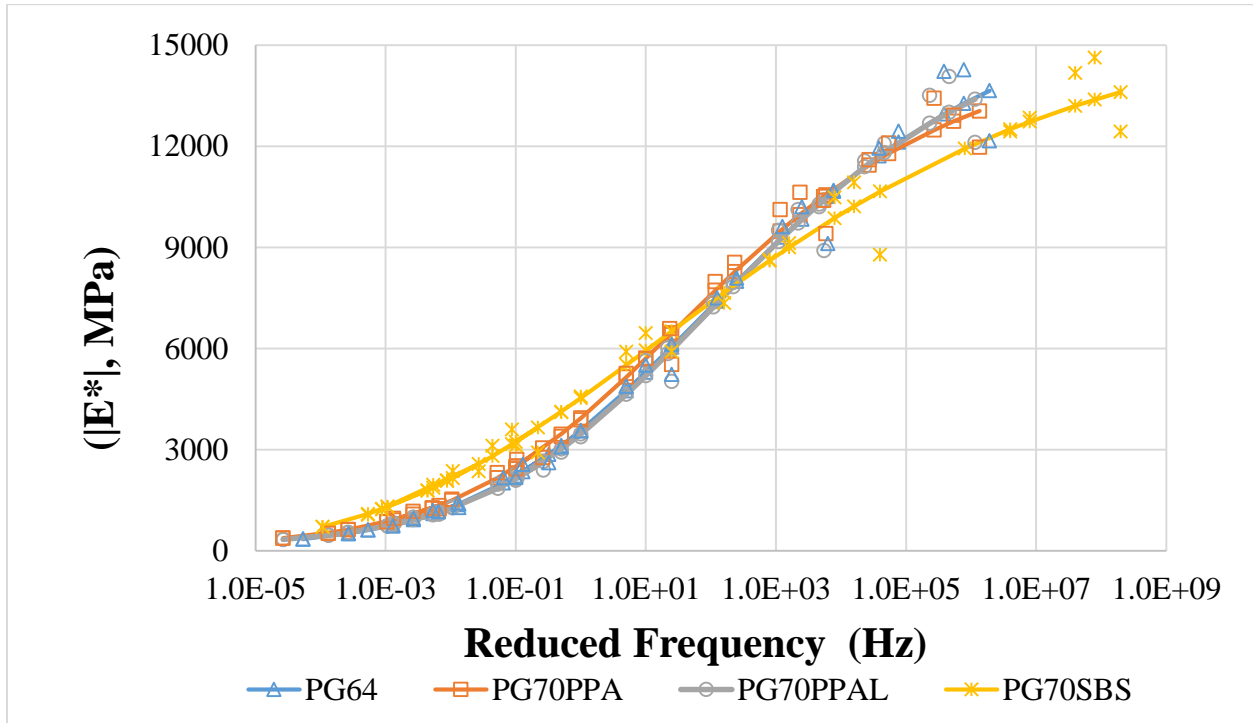


Figure 12. Uniaxial  $|E^*|$  Dynamic Modulus Master Curve

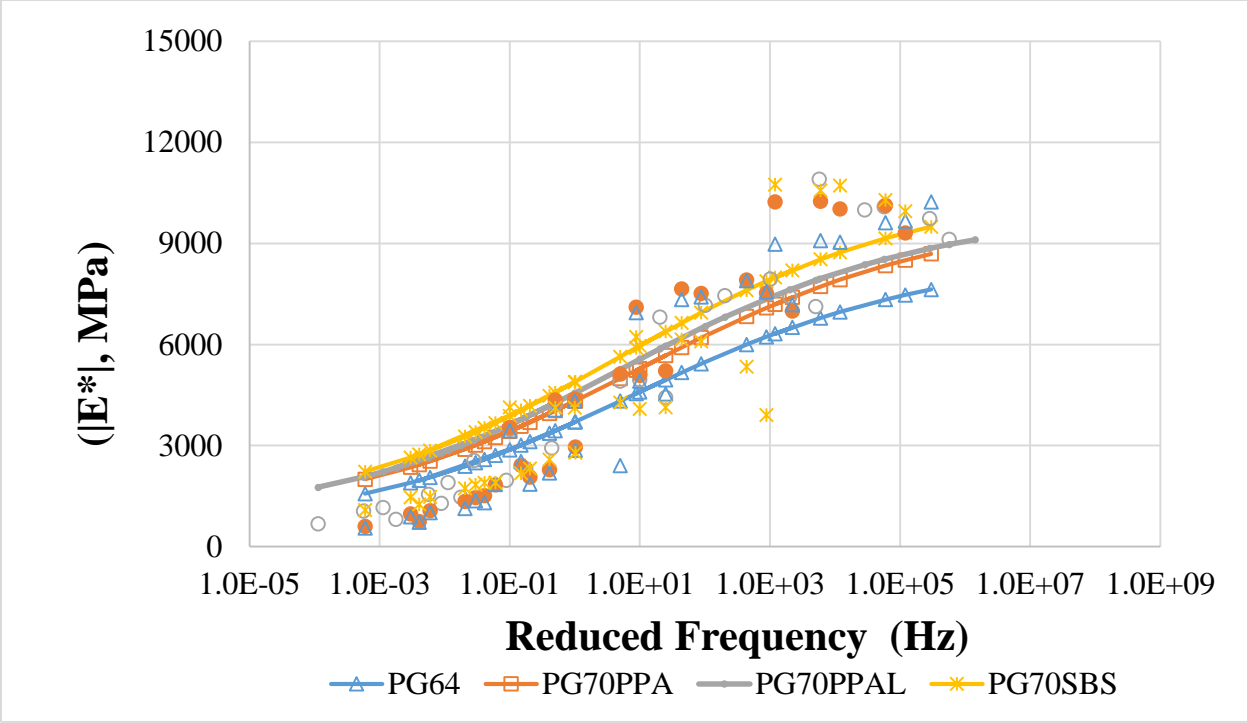


Figure 13. IDT  $|E^*|$  Dynamic Modulus Master Curve

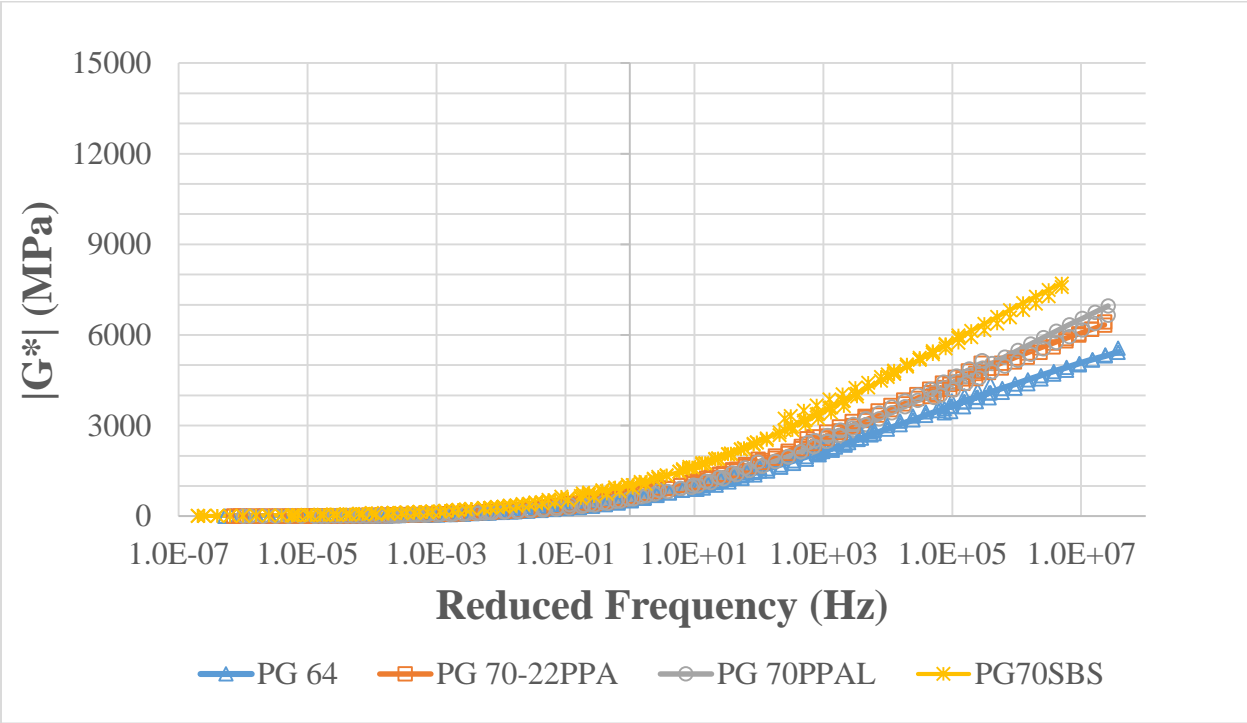
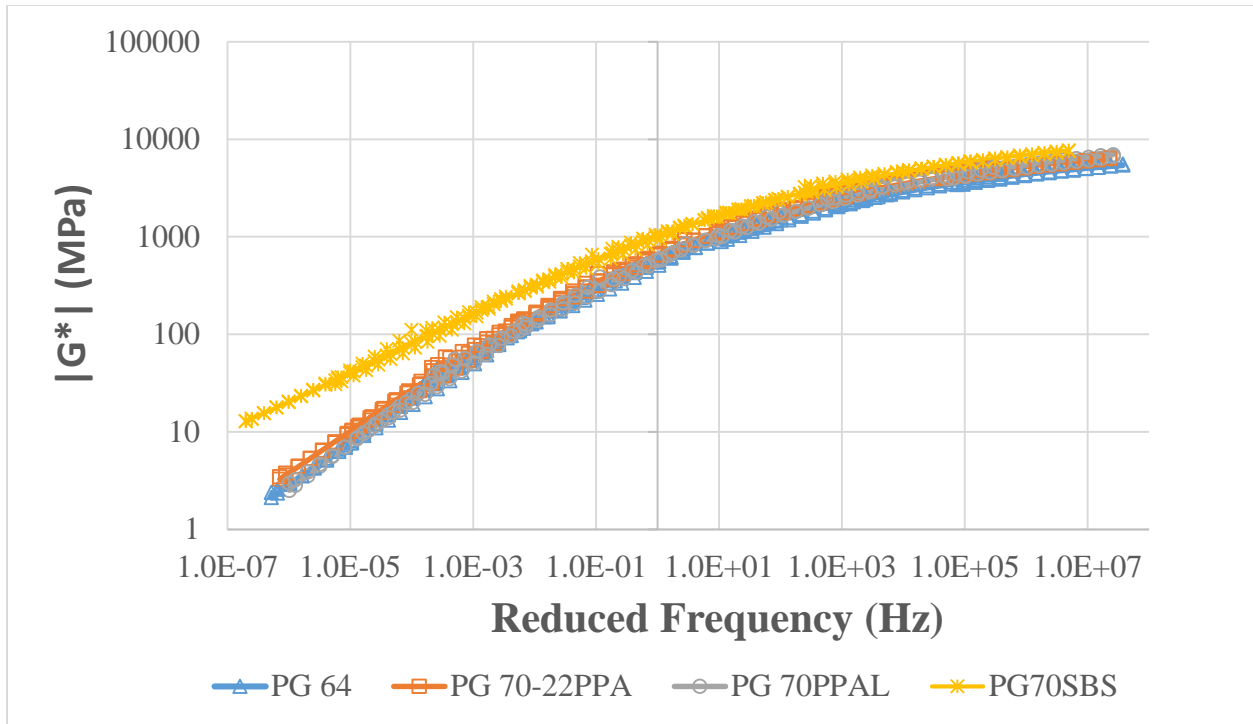


Figure 14. Torsion Bar  $|G^*|$  Master Curve



**Figure 15. Torsion Bar  $|G^*|$  in Log Configuration Master Curve**

## B. Black Space Diagram

For Uniaxial  $|E^*|$  dynamic modulus (Figure 16), for all four materials, there are not clear differences in stiffness, elasticity or viscosity. For IDT  $|E^*|$  (Figure 17), the four materials behave almost the same as Uniaxial  $|E^*|$ . Therefore, there are no differences in the properties that Black Space diagram shows. On the other hand, for Torsion Bar  $|G^*|$  (Figure 18), there are differences in elasticity and viscosity which are the properties related to complex shear modulus  $|G^*|$ . PG 64, PG70PPA, PG 70PPAL show to be a more viscous material. Nonetheless, PG70SBS is more elastic. The phase angle ranges between 3 and 26 degrees for Uniaxial  $|E^*|$ , between 0 and 33 for IDT  $|E^*|$  and from 6 to 55 degrees for Torsion Bar  $|G^*|$ .

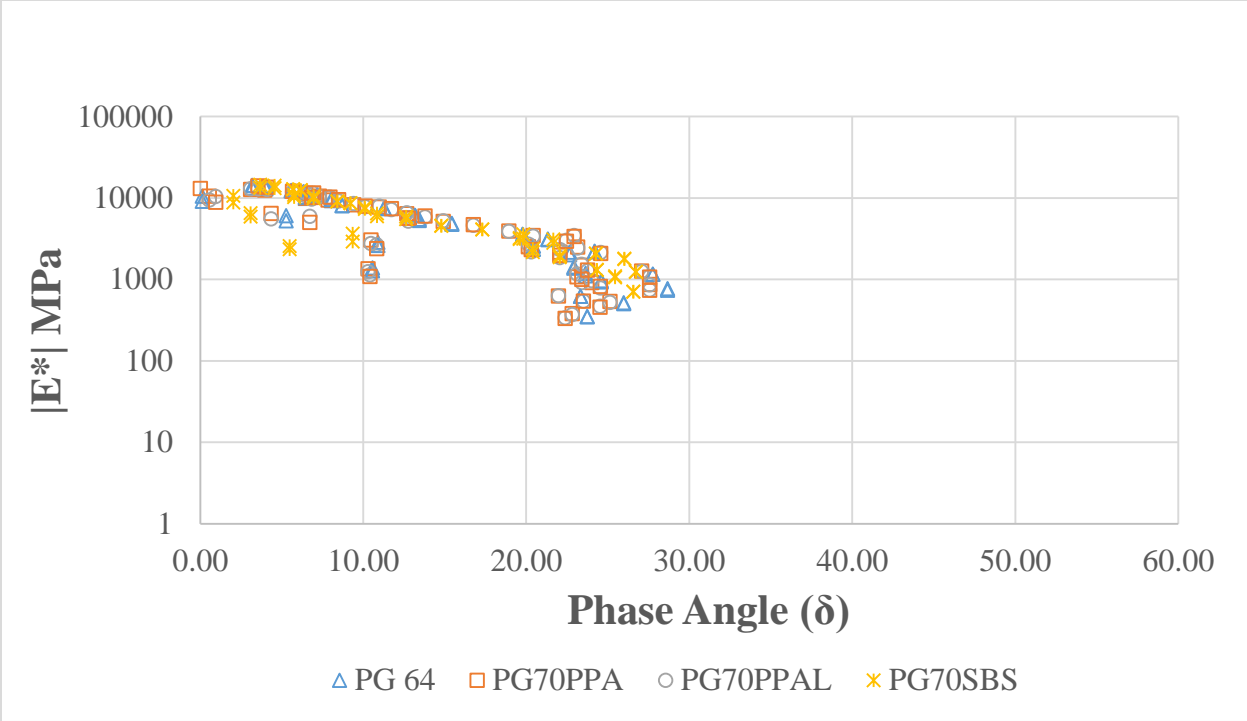


**Figure 16. Uniaxial |E\*| Dynamic Modulus Black Space Diagram**

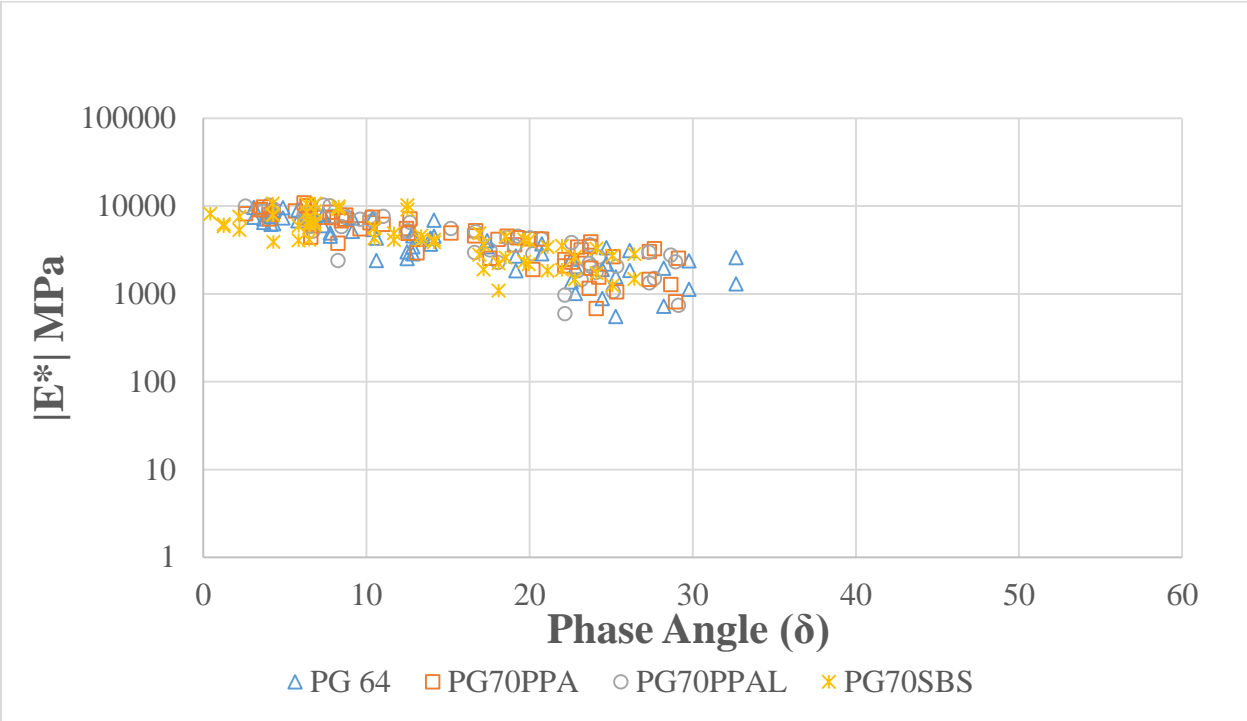


**Figure 17. IDT |E\*| Black Space Diagram**

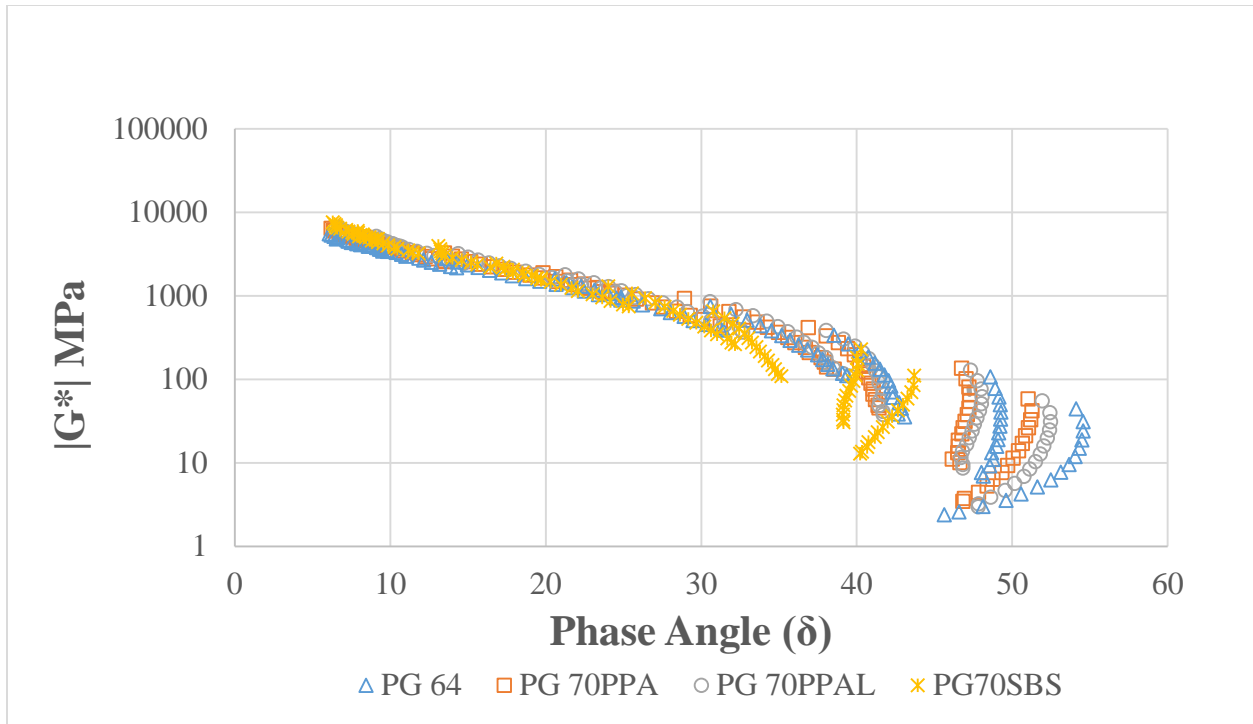


**Figure 18. Torsion Bar  $|G^*|$  Black Space Diagram**

### C. Statistical Test

For the comparison between the differences in the materials in each tests, ANOVA test was performed assuming that the data was normally distributed. The null hypothesis indicates that there is no significant difference between the materials, and the alternative hypothesis indicates that there is a significant difference between the materials. The program used to perform the data analysis was MiniTab. In order to make a comparison between the materials tested, another test was performed which measure multiple comparisons between materials named Tukey's Method.

The results showed (Table 3) that for master curves, Uniaxial  $|E^*|$  test had differences in PG70SBS material in the values of dynamic modulus with the other mixtures as is showed in the plotted master curve. For IDT  $|E^*|$  test, the values of dynamic modulus are similar between each other, so there are no differences. Finally, for Torsion Bar  $|G^*|$  test, Tukey's method showed differences

between PG70SBS and PG70PPAL, and between PG70SBS and PG64 in the values of shear modulus  $|G^*|$ . Therefore, the only materials that are similar are the PG70PPA and PG70PPAL.

**Table 3. ANOVA and Tukey’s Method for  $|E^*|$  Dynamic Modulus.**

<b>Test</b>	<b>Material</b>	<b>P-Value</b>	<b>Tukey’s Method</b>
<b>Uniaxial <math> E^* </math></b>	4 binder types	0.000	PG70SBS $\neq$ 3 binders
	Without SBS	0.221	All similar
<b>IDT <math> E^* </math></b>	4 binder types	0.199	All similar
<b>Torsion Bar <math> G^* </math></b>	4 binder types	0.000	PG70PPA = PG70PPAL

ANOVA and Tukey’s Method were also applied for the values of phase angle in Black Space diagram and showed the following results (Table 4): For Uniaxial  $|E^*|$  test, it shows differences in the degrees between PG70SBS and the other mixtures. Moreover, for IDT  $|E^*|$  test there are some differences between PG70SBS and the other mixtures. Finally, for Torsion Bar  $|G^*|$  test, there were significant differences between PG70SBS and PG64, and between PG70SBS and PG70PPAL. Therefore, the only materials that are similar are the PG64 and PG70PPAL.

**Table 4. ANOVA and Tukey's Method for phase angle.**

<b>Test</b>	<b>Material</b>	<b>P-Value</b>	<b>Tukey's Method</b>
<b>Uniaxial  E* </b>	4 binder types	0.005	PG70SBS ≠ 3 binders
	Without SBS	0.291	All similar
<b>IDT  E* </b>	4 binder types	0.004	PG70SBS ≠ PG70PPA PG70SBS ≠ PG70PPAL
	Without SBS	0.487	All similar
<b>Torsion Bar  G* </b>	4 binder types	0.000	PG64 = PG70PPAL

## V. Discussion

The results obtained clearly show how different results the three tests and both methods can bring. The four binder types behave in different ways also depending on its geometries. Uniaxial |E\*| and IDT |E\*| configurations presented almost same values between all four binder materials for Black Space diagram which was very difficult to evaluate the material about the elastic and viscous components of the asphalt compared with master curves. However, master curves show the clearly the characterization of the material by showing the property of stiffness. For instance, IDT |E\*| tended to have flatter curves than Uniaxial |E\*|, where the lowest and highest values of |E\*| were trimmed from the IDT |E\*|. Therefore, the Uniaxial configuration was able to provide more information about the lowest temperature/highest frequency and highest temperature/lowest frequency characteristics of asphalt pavement materials



Torsion bar  $|G^*|$  had much less information about the lowest temperature/highest frequency versus the two traditional tests, but provided much more information about the highest temperature/lowest frequency, which highlighted the potential benefits of SBS polymer modification versus the other three asphalt pavement materials. It also highlights that the torsion bar configuration and testing regime can give more information about the regions when the material behaves in a more viscous fashion versus elastic.

For Black Space diagram Torsion Bar  $|G^*|$ , there is a significant difference of four material's behavior when the phase angle is greater than  $30^\circ$ . This region is a transition between elastic dominated behavior ( $G' > 45^\circ$ ) and viscous dominated behavior ( $G'' > 45^\circ$ ). The unmodified binder PG64 shows the most viscous behavior, which indicates a higher susceptibility to rutting. While the PPA modified mixtures introduce more elastic behavior, the mixture with the highest elastic component is the SBS modified mixture. This shows that PPA may not be as capable of preventing rutting as SBS mixtures. However, in the lower phase angle regions, where the temperatures are lower and the loading rates are higher, the four mixtures show very similar behavior, indicating that fatigue cracking performance and low temperature cracking performance would be similar.

## **VI. Conclusions**

The purpose of this study was to make comparison between Uniaxial  $|E^*|$ , IDT  $|E^*|$ , and Torsion Bar  $|G^*|$  by plotting both master curves and Black Space diagram. Additionally, four binder materials were tested: PG64, PG70PPA, PG70PPAL, and PG70SBS. The results showed that there were differences between the test performed and the methods to assess the materials.

The conclusion in the finding of this study were the following:

- Black Space diagram is an effective tool that helps to assess material properties in order to compare stiffness, elasticity, and viscosity.
- The Black Space diagrams were similar for Uniaxial  $|E^*|$  and IDT  $|E^*|$ , but did not provide strong information about the elastic and viscous components of the asphalt pavement materials.
- PPA alone and combined with SBS showed to have properties of reducing rutting and cracking.
- The Black Space diagram of the Torsion Bar  $|G^*|$  showed more information than the two traditional tests: Uniaxial  $|E^*|$  and IDT  $|E^*|$ , with significant information about the viscous components (higher phase angle values, large  $G''$  component).
- SBS mixtures using the torsion bar  $|G^*|$  shows a clear difference of benefiting from rutting resistance.

## References

AASHTO (2014). Standard method of test for Determining Dynamic Modulus of Hot Mix Asphalt (HMA). *T 342-11*. Washington D.C.

AASHTO (2013). Standard method of test for Determining the Creep Compliance and Strength of Hot Mix Asphalt (HMA) Using the Indirect Tensile Test Device. *TP 322-07*. Washington D.C.

ASTM (2014). Standard method for Determining the Complex Shear Modulus ( $G^*$ ) of Bituminous Mixtures Using Dynamic Shear Rheometer. *ASTM D7552-09*. West Conshohocken, PA.

Baumgarder, G. (2010). Why and How of Polyphosphoric Acid Modification – An Industry Perspective. *Journal of the Association of Asphalt Paving Technologists*, 79, 663-678.

Bennert, T., Martin, J-V. (2010). Polyphosphoric Acid in Combination with Styrene-Butadiene-Styrene Block Copolymer - Laboratory Mixture Evaluation. *Journal of the Association of Asphalt Paving Technologists*, 79.

Behbahani, H., Aliha, M., Fazaeli, H., Rezaeifar, M. (2013). Effect of Characteristics Specifications on Fracture Toughness of Asphalt Concrete Materials. *13<sup>th</sup> International Conference on Fracture*.

Cao, W., Liu, S., Li, Y., Xue, Z. (2016). Rutting-Resistance Performance of SBS and Anti-Rutting Additive Composite-Modified Asphalt-Concrete Mixtures. *Journal of Testing and Evaluation*, 44, (2), 921-929.

Clyne, T., Johnson, E., McGraw, J., Reinke, G. (2012). Field Investigation of Polyphosphoric Acid-Modified Binders at MnRoad. TRB E-C160 January 2010, 115-130.

Di Benedetto, H., Olard, F., Sauzeat, C., Delaporte B. (2011). Linear Viscoelastic behavior of bituminous materials: From binders to mixes. *Road Materials and Pavement Design*.

Khattak, M., Baladi, G. (2013). Analysis of Fatigue and Fracture of Hot Mix Asphalt Mixtures. *Hindawi Publishing Corporation*.

Kim, J., Lee, H., Kim, N. (2010). Determination of Shear and Bulk Moduli of Viscoelastic Solids from the Indirect Tension Creep Test. *Journal of Engineering Mechanics*, 136 (9), 1067-1075.

Kim, R., Seo, Y., King, M., Momen, M. (2004). Dynamic Modulus Testing of Asphalt Concrete in Indirect Tension Mode. Transportation Research Record: Journal of Transportation Research Board, 1891, 163-173.

Li, X., Clyne, T., Reinke, G., Johnson, E., Gibson, N., Kutay, M. (2011). Laboratory Evaluation of Asphalt Binders and Mixtures Containing Polyphosphoric Acid. *Transportation Research Board*, 2210, 47-56.

- Mensching, D., Rowe, G., Daniel, J., Bennert, T. (2015). Exploring Low-Temperature Performance in Black Space. *Road Materials and Pavement Design*. 16, (2), 230-253.
- Mobasher, B., Mamlouk, M., Lin, H. (1997). Evaluation of Crack Propagation Properties of Asphalt Mixtures. *Journal of Transportation Engineering*. 123(5), 405-413.
- Naik, A., Biligiri, K. (2014). Predictive Models to Estimate Phase Angle of Asphalt Mixtures. *American Society of Civil Engineers*.
- Rastegar, R. (2016). Plant versus Laboratory Production: Impact on Measure Properties of Mixtures with RAP and RAS. *Transportation Research Board 2016 Annual Meeting Presentation*.
- Roberts, F., Kandhal, P., Brown, E., Lee, D., Kennedy, T. (1996). Hot Mix Asphalt Materials, Mixture Design and Construction. 2th Edition. *National Asphalt Pavement Association Research and Education Foundation*.
- Romero, P. (2013). Implementation of Low Temperatures Tests for Asphalt Mixtures to improve the Longevity of Road Surfaces. *Transportation Research Board*.
- Taherkhani, H., Collop, A.C. (2008). Determination of the Elastic Modulus and Poisson's Ratio of Asphaltic Mixtures Using Uniaxial Creep Recovery Tests. *Airfield and Highway Pavements*, 159-170.
- Timoshenko, S.P. (1953). *Theory of Elasticity*. 3<sup>rd</sup> Edition. McGraw Hill Book Co., New York, NY.
- Wagoner, M., Butlar, W., Paulino, G. (2005). Investigation of the Fracture Resistance of Hot-Mix Asphalt Concrete Using a Disk-Shaped Compact Tension Test. *Transportation Research Record: Journal of the Transportation Research Board, No 1929*, Washington, D.C, 183-192.
- Yang, S., Braham, A., Underwood, S., Hanz, A., Reinke, G. (2015). Correlating Field Performance to Laboratory Dynamic Modulus from Indirect Tension and Torsion Bar. *Journal of the Association of Asphalt Paving Technologists*.